Citation: Wijaya, A., M. Yamada (2022), Development of an earthquake early warning system in the western part of Java using a strong motion network, Synopsis of IISEE-GRIPS Master's Thesis.

DEVELOPMENT OF AN EARTHQUAKE EARLY WARNING SYSTEM IN THE WESTERN PART OF JAVA USING A STRONG MOTION NETWORK

Angga Wijaya[1] **Supervisor: Masumi YAMADA**[2]
MEE21702

ABSTRACT

The development of an earthquake early warning system (EEWS) has been done by applying the extended integrated particle filter (IPFx) method using a strong ground motion network in the western part of Java, Indonesia. The method was applied to continuous waveforms including 95 earthquakes (M > 4 and seismic intensity ≥ II MMI) and to the one-day waveforms including the 2022 Banten earthquake sequences. We used 190 stations divided into 99 conventional force-balanced accelerometer sensors (FBA) and 91 Micro-Electro-Mechanical System (MEMS) sensors. Early warning criteria were given when the number of picks was more than five and the maximum seismic intensity was ≥ 3.5 (IV MMI) based on the seismic attenuation equation. This system has successfully detected 95 earthquakes and provided warnings to 46 from 49 events with observed seismic intensity ≥ 3.5 MMI. The system also successfully detected five earthquakes of magnitude ≥ 4.0 as converged earthquakes and provided warnings to two events with an observed seismic intensity of ≥ 3.5 for the 2022 Banten earthquake sequence. The IPFx method shows good accuracy to estimate earthquake source locations with median errors of 12 km, 22.7 km, 0.27, and 0.62 for the epicenter, depth, magnitude, and seismic intensity, respectively, relative to the Indonesia Agency for Meteorology, climatology, and Geophysics (BMKG) catalog. The system takes 3.4 seconds after the first P-wave was detected, and it is 6 seconds faster than the previous method tested by BMKG. Based on the good accuracy and speed in estimating earthquake sources, the IPFx method has the potential to be developed into an earthquake early warning system in Indonesia in the future.

Keywords: Earthquake early warning, earthquake source, IPFx method.

1. INTRODUCTION

The development of an EEWS in Indonesia began with a collaboration between the Institute of Care-Life (ICL) from China and BMKG in 2019 as a pilot stage by installing 197 sensors along the island of Sumatra to Central Java. At the same time, BMKG is trying to self-develop an EEWS by adding 94 MEMS accelerometer sensors to the strong motion network in the West Java Region. The system was designed with several improvements in the Taiwan regional EEW system (eBEAR). Both systems currently show that there were still missed earthquakes and low accuracy of earthquake sources. We aim to develop an earthquake early warning system with a strong motion network in Indonesia by implementing the extended IPF (IPFx) method by Yamada et al. (2021). The IPFx method has the advantage of separating the phases of multiple earthquakes and having high accuracy in estimating earthquake sources. In addition, it also takes a shorter time to detect earthquakes. The performance of the method was evaluate based on the system's ability to detect and provide warnings for earthquakes with an intensity of more than 3.5 (IV MMI) with allowed the seismic intensity error ±1. We also

[1] Meteorological, Climatological, and Geophysical Agency (BMKG), Indonesia.
[2] Assistant Professor, Disaster Prevention Research Institute (DPRI), Kyoto University.

analyzed the accuracy of the earthquake source estimation by comparing the IPFx method catalog with the BMKG catalog.

2. DATA

This study used continuous waveform data from the BMKG strong motion network in the western part of Java, as many as 190 stations with three components consisting of 99 FBA accelerometers and 91 MEMS accelerometers, as shown in Figure 1. The instruments used in the FBA network are TSA-100 (Metrozet), Titan (nanometrics), and G210S (Meisei Electrics), which has a sampling rate of 100Hz with a resolution of 24 bits. Meanwhile, the MEMS accelerometer, P-Alert plus (Sanlien) with a sampling frequency of 100 Hz and a resolution of 16 bits, was also used. Earthquake data used in this study were 95 events between January 1, 2020, and March 30, 2022, with a magnitude greater than 4.0, as shown in Figure 1. Stations with a data loss of more than 15 seconds during an earthquake or a clock error were not included in the simulation. Simulations were also carried out with a one-day continuous waveform on January 14, 2022, during the Banten Earthquake (M6.7).

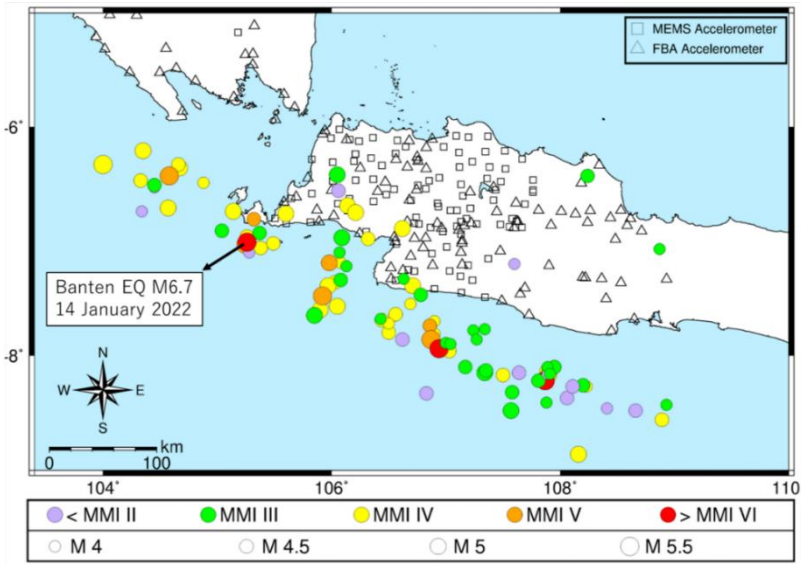

Figure 1. Seismic station and earthquake distribution used in this study.

3. METHODOLOGY

3.1. Extended IPF Method

The IPFx method is a new source estimation algorithm updated from the IPF method (Tamaribuchi et al., 2014) for EEWS enhancement (Yamada et al., 2021). This method has two steps: single station processing for every station and network processing for centralized event detection and source estimation. This method can analyze multi-events simultaneously with several predetermined conditions based on the amplitude and P-wave arrival time data.

In the single station processing every one-second accelerometer data was processed by eliminating the DC offset and instrument response (Yamada et al., 2014). P-wave detection was carried out by applying the Tpd method (Yamada and Mori., 2022) after applying a second-order bandpass filter with a corner frequency of 5-10 Hz to eliminate the effects of noises. Furthermore, the amplitude parameter was extracted in the form of maximum vertical velocity, maximum vertical displacement, and amplitude (the sum of the three component vectors) of acceleration, velocity, and displacement. The information was used for multiple definitions of magnitudes.

The trigger information obtained from single station processing was transmitted to network processing to detect new earthquakes and estimate earthquake sources. When a new trigger was observed

and does not match the existing event, it will be categorized as an EQp (pending earthquake), which may be a P-wave from a potential earthquake. If there are multiple triggers close to the first trigger (at least 3 triggers), the earthquake was converted into EQ (ongoing earthquake), and the earthquake source estimation begins. The location of the EQ was estimated and updated every second. The source parameters were estimated using the IPF method (Wu et al., 2014) with a Bayesian Inference approach where the initial hypocenter is the center of the Voronoi cell from the first trigger. The number of stations used for the source estimation was defined by the estimation group. The estimation group includes the 20 closest stations from the first trigger station and 10 additional stations with wide azimuthal coverage. The EQ was converted into EQc (converged earthquake) when the source parameters become stable.

3.2. Seismic Intensity Estimation

In this study, the intensity estimation becomes essential to decide which earthquake warning information was disseminated to the public. The warning criteria used the number of picks more than five and seismic intensity (SI) estimation greater than 3.5 (IV MMI). Intensity estimation used the converted peak ground acceleration (PGA) by equation from Wald (1999). The PGA calculation in this study followed the ground motion prediction equation (GMPE) used by BMKG in producing the shakemap. Two formulas were used depending on the depth identified as the interface, crustal or slab earthquakes, and the earthquake magnitude. The GMPE in Zhao et al. (2006) was used for deep earthquakes with a depth of more than 50 km or large earthquakes with a magnitude of more than 5.3. The GMPE in Akkar and Boomer (2007) was used for small and shallow earthquakes (depth < 50 km and magnitude < 5.3).

4. RESULTS AND DISCUSSION

4.1. System performance

The results showed that the IPFx method detected all 95 earthquakes divided into groups : (1) 43 events that succeeded in providing the warnings (observed seismic intensity ≥ 3.5 and estimated seismic intensity ≥ 3.5- Δ1.0), (2) three that failed to give a warning (underestimated seismic intensity), (3) three were false alarms (overestimated seismic intensity), and (4) 46 events that succeeded to not giving a warning (observed seismic intensity < 3.5 and estimated seismic intensity < 3.5+Δ1.0). The system took an average of 3.4 seconds to detect earthquake events after the first P-wave detection or 16.8 seconds after the origin time. Since the earthquakes mostly occurred off the southern coast of the island of Java

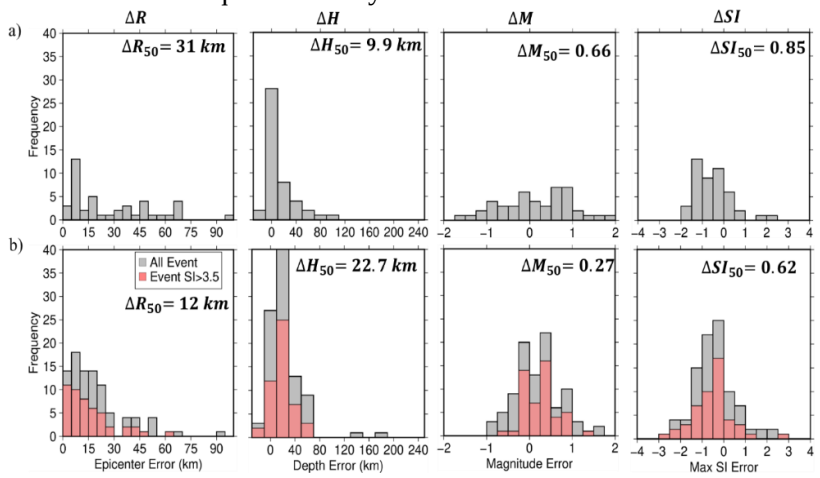

Figure 2. Histograms of epicenter, depth, magnitude, and SI errors in first warning catalog for earthquake with SI ≥ 3.5 (a) and final catalog (b). Red histogram in (b) shows the parameters error for earthquake with SI ≥ 3.5. The top-right numbers in each histrogram show the median error for IPFx method compared with BMKG catalog.

and in the Sunda Strait, the time to detect earthquakes was longer than that of the shallow inland

earthquakes. Our results showed the earthquake was detected 17.5 seconds after the origin time, and 7.5 seconds for inland earthquakes.

Figure 2 shows the accuracy of the earthquake source parameters from the estimation results of 95 earthquakes using the IPFx method, compared with the BMKG earthquake catalog. Figure 2a represents the accuracy of the initial earthquake parameters obtained when the system gave the warning. In the histogram, 50% of events have errors of 31 km, 9.9 km, 0.66, and 0.85 for the epicenter, depth, magnitude, and seismic intensity, respectively. In addition, the location of the earthquake source is reasonably accurate, although there are still more than 50% of events with errors > 30km. Figure 2b shows the accuracy of earthquake parameters in the final catalog. The final source parameters estimated by the IPFx method were improved, especially for the epicenter and magnitude, where 50% of events had errors of 12km and 0.27, respectively. In addition, in the histogram, the epicenter of the 79% earthquake has an error of <30 km.

4.2. Comparison IPFx and eBEAR method

We compared the current system with the previously tested EEWS, the eBEAR method. We used 12 earthquakes in 2022 with an observed intensity of ≥ 3.5 for the comparison. Figure 3 shows an example of the mainshock of the 2022 Banten earthquake. It shows the difference in the accuracy of the earthquake parameters of the two methods. The hypocenter location of the IPFx method is closer to the BMKG catalog than the eBEAR method. Based on the time history of the earthquake parameters, the IPFx method can detect the earthquake and provide an early warning 12 seconds faster.

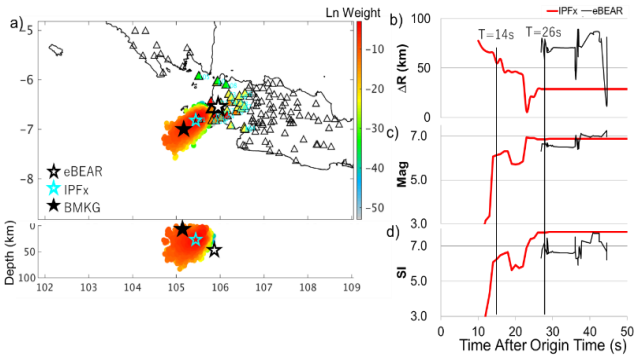

Figure 3. Result of the Banten Mainshock on January 14, 2020, with magnitude 6.7 and SI 7.5 (VIII MMI). a) Estimated source location at converged time. Black, blue, and white stars, respectively, indicate the source location for BMKG catalog, IPFx, and eBEAR. The colored and white triangles, respectively, indicates the triggered and non-triggered stations in estimation group. (b)-(d) Time history of estimated earthquakes parameters after origin time. Red and black lines, indicate the result of IPFx method and eBEAR method. The vertical black lines indicate time of earthquake warning. (b) epicenter error, (c) magnitude, (d) seismic intensity.

The comparison of earthquake detection speed is shown in Figure 4. The average time to issue earthquake warnings by the IPFx method after detecting the first P-wave was 3.4 seconds, and 17.6 seconds after the origin time. Meanwhile, the eBEAR method took 10.2 seconds after the first P-wave detection and 23.5 seconds after the origin time. It showed that the IPFx method was 6 seconds faster than the eBEAR method.

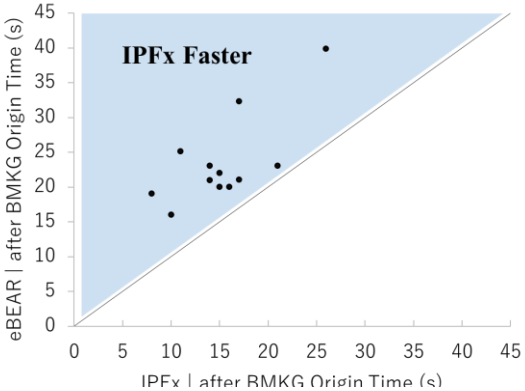

Figure 4. Time of first event detection after origin time for IPFx and eBEAR.

4.3 Example of Incorrect Earthquake Source Estimation

Figure 5 shows an example of earthquakes with incorrect epicenter estimation. The left example is an earthquake on July 28, 2020. It shows a large error in the earthquake hypocenter estimation from the IPFx method. The MEMS sensor marked by red boxes failed to detect the P wave due to weak ground

motions and low sensitivity of the MEMS sensors, and then the S-wave was detected and treated as the P-wave arrival time for earthquake source estimation.

The right figure shows an example of the earthquake on January 27, 2020. The estimated earthquake source was far from that of the BMKG catalog. Due to this location error, SI was underestimated. The error was caused by the poor quality of the accelerograms on the distant FBA sensor. The triggers were caused by noises before the P-wave arrivals which moved the estimated source farther offshore than the actual location.

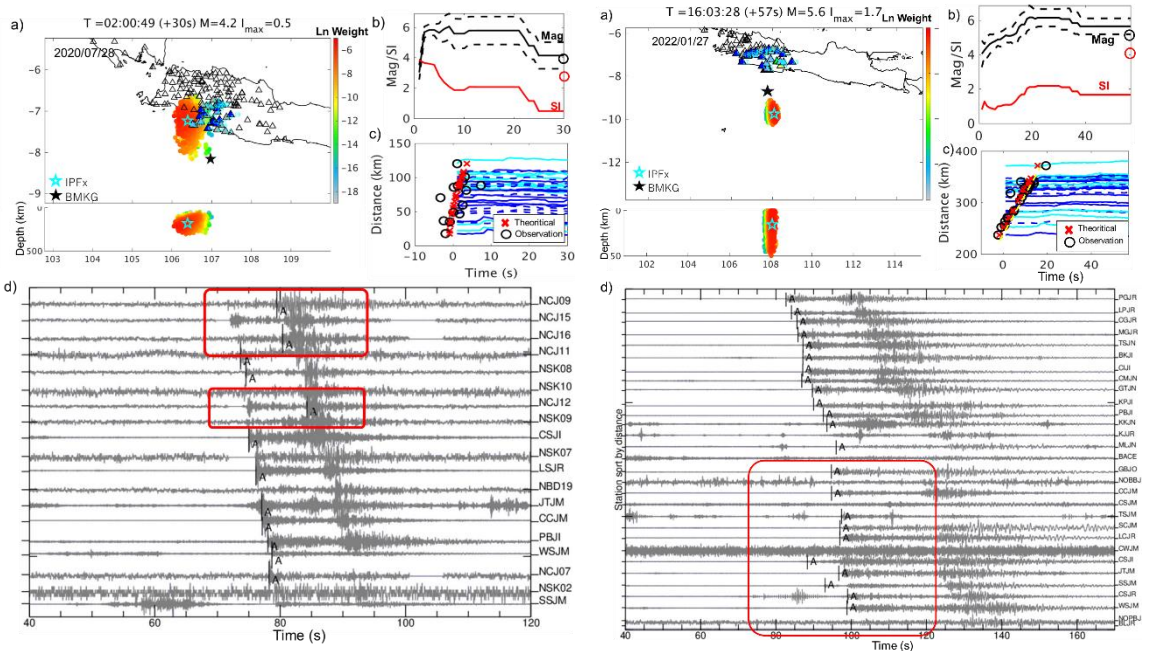

Figure 5. Result of 28 July 2020 (left) and 27 January 2022 (right) earthquakes. (a) the location of the earthquake source where the blue and black stars indicate the optimal location of the IPFx and BMKG catalog estimates, respectively. (b) the time history of magnitude (black line) and seismic intensity (red line) after the detection time. The black and red circles indicate the magnitude and seismic intensity from the BMKG catalog. (c) Comparison of the theoretical and observed P-wave arrival times from the IPFx method. Blue lines indicate the envelope signal after the first detection time. (d) waveforms of the earthquake with 'A' as P-wave arrivals and the red box indicates the bad detection (left) and the noisy signal (right).

4.4. Performance comparison of different strong motion network

We tried to compare the effect of sensor type by simulating one-day waveform data with three different stations groups, FBA Accelerometer only, MEMS Accelerometer only, and a combination of the two sensors (FBA+MEMS). The simulation results show that seven events, three events, and five events were detected by FBA, MEMS, and combined sensor networks, respectively.

Table 1. Average errors of epicenter, magnitude, and detection time after the origin time for the different seismic networks.

Network Type	ΔR (km)	ΔM	Detection Time (s)
FBA	5.6	0.3	17.3
MEMS	54.2	0.7	13.8
FBA+MEMS	9.6	0.33	12.1

Table 1 compares the accuracy of the three earthquakes detected with three types of seismic networks. The result of the FBA sensor only showed higher accuracy for epicenter error. On the other hand, the average detection time after the origin time was 17.3 seconds, 13.8 seconds, and 12.1 seconds for FBA only, MEMS only, and combined seismic networks, respectively. The station density and sensor noise level greatly influenced the detection time and accuracy.

5. CONCLUSIONS

The IPFx method showed a good performance to detect 95 earthquakes with reasonable accuracy. Forty-three earthquakes above the warning criterion (seismic intensity ≥ 3.5) were successfully identified as a large event (estimated seismic intensity ≥ 3.5- Δ1.0), 46 earthquakes under the warning criterion were successfully estimated as a small event (estimated seismic intensity < 3.5+Δ1.0), three events failed to give a warning (underestimated seismic intensity), and three events were false alarms (overestimated seismic intensity). This system could detect events 3.4 seconds after the first P wave was detected, 17.5 seconds after the origin time for offshore earthquakes, and 7.5 seconds for inland earthquakes. Our results showed that the IPFx method had median errors of 31 km, 9.9 km, 0.66, and 0.85 for the epicenter, depth, magnitude, and seismic intensity, respectively. The final catalog showed that 76 of the 95 earthquakes had an epicenter error of < 30 km, and 65 events had an absolute error of seismic intensity less than 1. The comparison of the performance of the IPFx method with the eBEAR method showed the IPFx method had an average epicenter error of 24.95 km, while the eBEAR method was 59.59 km. In addition, the IPFx method was 6 seconds faster in detecting and providing earthquake warnings than the eBEAR method.

We conclude that the IPFx method has the potential to be developed as an earthquake early warning system in Indonesia using the BMKG strong motion network. This system can improve the accuracy and speed of detecting and providing earthquake warnings. While there were limitations to the IPFx method caused by the poor quality of the accelerometer data from the FBA sensor and the difference in the sensors used, the MEMS sensor with low sensitivity cannot correctly record weak earthquake motion.

ACKNOWLEDGEMENTS

This research was conducted during the individual study period of the training course “Seismology, Earthquake Engineering and Tsunami Disaster Mitigation” by the Building Research Institute, JICA, and GRIPS. I would like to express my deep gratitude to my supervisor, Masumi Yamada, Ph.D. from Kyoto University for her valuable support, experience, and knowledge to use the IPFx programs during my individual study. I would also like to acknowledge Dr. Takumi Hayashida for his permanent support from the beginning to the end of the program.

REFERENCES

Akkar, S., and J. J. Bommer., 2007b, Bulletin of the Seismological Society of America 97 (2), 511–530.
Tamaribuchi, K., Yamada, M., and Wu, S., 2014, Zisin 67, no. 2, 41–55.
Wald D. Quitoriano V. Dengler L. Dewey J., 1999, Seismol. Res. Lett. 70, 680–697.
Wu, S., M. Yamada, K. Tamaribuchi, and J. Beck., 2014, Geophys. J. Int. 200, no. 2, 791–808.
Yamada, M., Tamaribuchi, K. & Wu, S., 2014, J. Japan Assoc. Earthq. Eng., 14, 21–34.
Yamada, M., Tamaribuchi, K., & Wu, S., 2021, Bulletin of the Seismological Society of America, 111 (3), 1263-1272.
Yamada, M., & Chen, D. Y, 2022, Terrestrial, Atmospheric and Oceanic Sciences, 33 (1), 1-10.
Yamada, M., & Mori, J., 2022, Geophysical Journal International, 228 (1), 387-395.
Zhao, J.X., Zhang, J., Asano, A., Ohno, Y., Oouchi, T., Takahashi, T., Ogawa, H., Irikura, K., Thio, H.K., Somerville, P.G. and Fukushima, Y., 2006, Bulletin of the Seismological Society of America, 96 (3), 898-913.